

Dalton Transactions

Accepted Manuscript

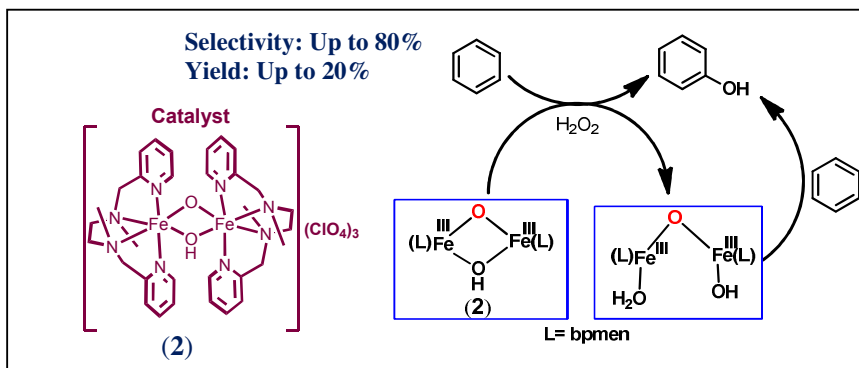


This is an *Accepted Manuscript*, which has been through the Royal Society of Chemistry peer review process and has been accepted for publication.

Accepted Manuscripts are published online shortly after acceptance, before technical editing, formatting and proof reading. Using this free service, authors can make their results available to the community, in citable form, before we publish the edited article. We will replace this *Accepted Manuscript* with the edited and formatted *Advance Article* as soon as it is available.

You can find more information about *Accepted Manuscripts* in the [Information for Authors](#).

Please note that technical editing may introduce minor changes to the text and/or graphics, which may alter content. The journal's standard [Terms & Conditions](#) and the [Ethical guidelines](#) still apply. In no event shall the Royal Society of Chemistry be held responsible for any errors or omissions in this *Accepted Manuscript* or any consequences arising from the use of any information it contains.





Journal Name

ARTICLE

Aromatic Hydroxylation by an Oxo-bridged Diiron(III) Complex: A Bio-inspired Functional Model of *Toluene Monooxygenases*

Received 00th January 20xx,
Accepted 00th January 20xx

DOI: 10.1039/x0xx00000x

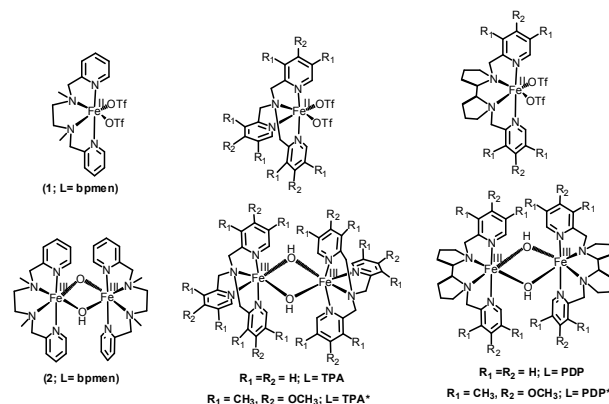
www.rsc.org/

Ambica Kejriwal,^a Pinaki Bandyopadhyay^a and Achintesh N. Biswas^{*b}

In biology, aromatic hydroxylation is carried out by a family of heme and nonheme oxygenases, such as *cytochrome P450*, *toluene monooxygenases* (TMOs), methane monooxygenases (MMO). In contrast, a vast majority of synthetic iron based catalysts employed so far in aromatic hydroxylation are monomeric in nature. Herein, we have employed a diferric complex of an aminopyridine ligand, $(((\text{bpmen})_2\text{Fe}_2\text{O}(\mu\text{-O})(\mu\text{-OH}))(\text{ClO}_4)_3$ (**2**), bpmen = N,N'-dimethyl-N,N'-bis(2-pyridylmethyl)-1,2-diaminoethane) towards aromatic hydroxylation with H_2O_2 and acetic acid. The diiron(III) complex shows promising reactivity in hydroxylation of benzene and alkylbenzenes with a higher selectivity towards aromatic ring hydroxylation over alkyl chain oxidation. The μ -oxo diiron(III) core has been shown to be regenerated at the end of catalytic turnover. However, mechanistic studies indicate that the diiron(III) complex undergoes dissociation into its monomeric congener and the resulting iron(III) complex mitigates aromatic hydroxylation.

Introduction

Selective hydroxylation of aromatic C-H bonds in a single step is a subject of paramount interest in synthetic chemistry.¹ Till to date, development of effective one step process for the conversion of aromatic compounds into their hydroxyl derivatives has remained elusive, primarily due to the oxidant resistant nature of the aromatic compounds.² For example, oxidation of benzene to phenol in large scale is achieved by the proton catalyzed cleavage of cumene hydroperoxide, which also yields acetone as a significant by-product.³ Moreover, this cumene process is energy intensive and produces phenol in only 5% overall yield. Thus, development of single step, selective and co-product free process for aromatic hydroxylation under ambient condition remains a challenging task for the synthetic chemists.⁴ However, the ability of several metalloenzymes to catalyze aromatic hydroxylation using dioxygen provides necessary impetus to the chemists to design suitable metal catalysts for activating C(aryl)-H bonds. In nature, aromatic hydroxylation is catalyzed mainly by iron containing monooxygenases and dioxygenases. In particular, the diiron hydroxylases such as *methane monooxygenase* (sMMO), *toluene-4-monooxygenases* (T4MO) exhibit remarkable catalytic reactivity towards aromatic hydroxylation.⁵



Scheme 1 Structures of mononuclear and dinuclear iron complexes based on aminopyridine ligands

Model systems have been developed in parallel to contribute the understanding of their mechanisms of action and eventually to mimic their activities. In particular, several iron(II) complexes have emerged as promising catalysts to affect aromatic hydroxylation with activated oxygen surrogate such as hydrogen peroxide.⁶⁻¹⁰ Among them, the iron(II) complex $[\text{Fe}^{\text{II}}(\text{bpmen})(\text{CH}_3\text{CN})_2](\text{ClO}_4)_2$ (**1**; bpmen = N,N'-dimethyl-N,N'-bis(2-pyridylmethyl)-1,2-diaminoethane, Scheme 1) has emerged as one of the most successful mononuclear iron-based catalyst in promoting aromatic hydroxylation with H_2O_2 and acetic acid.⁷

In this case, the authors identified the formation of an Fe(III)-OOH species, which is proposed to generate a highly active oxoiron species *via* an acid-assisted O-O cleavage.^{7a} The inability of independently generated bpmen-Fe^{IV}=O in promoting aromatic hydroxylation led the authors to propose

^a Department of Chemistry, University of North Bengal, Raja Rammohunpur, Siliguri 734013, India. Fax: 91 353 2699001; Tel: 91 353 277684; E-mail: pbchem@rediffmail.com

^b Department of Chemistry, Siliguri College, Siliguri 734001, India; E-mail: achintesh@gmail.com

† Footnotes relating to the title and/or authors should appear here. Electronic Supplementary Information (ESI) available: [details of any supplementary information available should be included here]. See DOI: 10.1039/x0xx00000x

a putative iron(V)-oxo as the true oxidant. Indeed, a highly reactive and unstable species in $1/H_2O_2/AcOH$ system was observed at -70° to $-80^\circ C$ by Talsi *et al.* and they assigned the $S=1/2$ species as $[(bpmen)Fe^V=O(OC(O)CH_3)]^{2+}$.¹¹ However, the identity of this species as oxoiron(V) is questioned by Oloo *et al.* and they argued in favour of a low-spin acylperoxoiron(III) species based on its EPR, resonance raman and Mössbauer data.¹² Thus, the identity of the true oxidant in aromatic hydroxylation by $1/H_2O_2/AcOH$ system remains speculative till to date. Very recently, Talsi and co-workers have provided convincing EPR evidence supporting the formation of a formal oxoiron(V) species from dinuclear iron(III) complexes (bearing aminopyrine ligands TPA* and PDP*, TPA*=tris(3,5-dimethyl-4-methoxypyridyl-2-methyl)amine, PDP*=bis(3,5-dimethyl-4-methoxypyridyl-2-methyl)-(S,S)-2,2'-bipyrrrolidine, Scheme 1) with H_2O_2 and acetic acid.¹³ In presence of acetic acid, the dinuclear iron(III) complexes are shown to get converted into monomeric ferric complexes of the type $[(L)Fe^{III}(\kappa^2-(OC(O)CH_3)_2)]^{2+}$, which, reacts with H_2O_2 to generate formally oxoiron(V) intermediate [either $(L)Fe^V=O$ or $(L^{*+})Fe^{IV}=O$]. The results encouraged us to investigate the reactivity of diferric complex of bpmen, $[(bpmen)_2Fe_2O(\mu-O)(\mu-OH)](ClO_4)_3$ (**2**) towards aromatic hydroxylation with H_2O_2 and AcOH. The crux of the present investigation is to examine whether the catalyst retains its μ -oxo diiron(III) core during catalytic turnovers. Given the structural similarity of the bpmen ligand to that of PDP*, formation of putative oxoiron(V) species in $1/H_2O_2/AcOH$ is envisioned. However, unlike TPA* and PDP*, absence of the electron-donating groups in bpmen may stabilize the diiron core in solution. In this contribution, we have explored the aromatic hydroxylation ability of the diiron(III) complex (**2**) with H_2O_2 at room temperature. Complex **2** has been found to promote aromatic hydroxylation and its reactivity is strikingly similar to its monomeric congener. However, unlike $1/H_2O_2/AcOH$ catalytic system, intermediacy of iron(III)-OOH species is not observed in aromatic hydroxylation by $2/H_2O_2/AcOH$, which indicates that a somewhat different mechanistic pathway is operative in this case.

Experimental

Materials and Instrumentation

All reagents and chemicals were purchased from sigma Aldrich and were used without further purification unless noted otherwise. 2-picolyl chloride, N,N'-dimethylethylenediamine and $Fe(ClO_4)_3 \cdot xH_2O$ were purchased from Sigma Aldrich. HPLC grade acetonitrile (S.D. Fine Chem. Ltd., India) and ethanol (E. Merck, India) were distilled over CaH_2 .¹⁴ H_2O_2 (as ~30% solution in water) was used as received and the exact active oxygen content of the oxidant was determined iodometrically prior to use.

UV-Vis spectra were recorded on an Agilent 8453 Spectrophotometer. Elemental Microanalysis (CHN) was done in Vario EL-III elementary analyser. The 1H NMR spectrum was

recorded on a Bruker spectrometer operating at 300 MHz. The product analyses were done by Perkin Elmer Clarus-500 GC with FID (Elite-I, Polysiloxane, 15-meter column). ESI-MS data were collected on a MICROMASS QUATTRO II triple quadrupole mass spectrometer.

Synthesis of the ligand bpmen and the complex $[(bpmen)_2Fe_2O(\mu-O)(\mu-OH)](ClO_4)_3$ (**2**)

The ligand bpmen (bpmen = N,N'-dimethyl-N,N'-bis(2-pyridylmethyl)-1,2-diaminoethane) was synthesized following the literature method.¹⁵ 1H NMR (300 MHz, $CDCl_3$): δ = 2.27 (s, 6H, -N-CH₃), 2.66 (s, 4H, -CH₂-CH₂-), 3.69 (s, 4H, N-CH₂-Py), 7.1-8.54 (m, 8H, Py ring).

The synthesis of the metal complex was carried out according to the published procedure.¹⁶ ESIMS: m/z: 392 (100%) $[M-2ClO_4]^{+2}$.

Reaction Conditions for catalytic experiments

A total of 20 μ L of a 1.0 M H_2O_2 solution (diluted from a 30% H_2O_2 solution) in CH_3CN was delivered all at once in air to a CH_3CN solution (2.0 mL) containing iron 1 mM catalyst and 300 mM aromatic substrate. The final ratio is catalyst: substrate: oxidant=1:300:10. In various experiments, acetic acid (1 equiv *w.r.t.* the catalyst) was added to the initial solution prior to the addition of oxidant. The solution was stirred for 15 mins. In all cases, the resulting solutions were treated with acetic anhydride (1.0 mL) together with 1-methylimidazole (0.1 mL) to esterify the diol products. Iodopentafluorobenzene was added as an internal standard. Organic products were extracted with $CHCl_3$, and the solution was washed with 1M H_2SO_4 , sat. $NaHCO_3$, and H_2O . The organic layer was dried with $MgSO_4$ and the solution was subjected to GC analysis. The products were identified by comparison of their GC retention times with those of authentic compounds. All experiments were run at least in duplicate, the reported data being the average of these reactions.

Kinetic Measurements

Kinetic measurements were performed in the UV-Vis spectrophotometer using **2** as catalyst with 300 mM benzene and hydrogen peroxide (10 mM) at 298 K. The formation of the 650 nm band was monitored with time. The experimental data fitting and calculation of the rate constants were performed by Origin 9.0 software. The activation enthalpy and entropy for hydroxylation of benzene were calculated from Eyring plot.

Results and discussion

Catalytic aromatic hydroxylation by complex **2**/ H_2O_2

The diiron(III) complex $[(bpmen)_2Fe_2O(\mu-O)(\mu-OH)](ClO_4)_3$ (**2**), is stable in air and is known to undergo ring opening in presence of water.¹⁶ The reactivity of complex **2** towards oxidation of arenes with mild H_2O_2 at room temperature has been evaluated. In a typical reaction, complex **2** (1.0 mM) is dissolved in anhydrous acetonitrile at 298K, benzene (300 equiv. *w.r.t.* **2**) is added and the reaction is initiated by adding H_2O_2 (10 equiv. *w.r.t.* **2**). After stirring the reaction mixture for

Journal Name

ARTICLE

Table 1. Aromatic hydroxylation catalyzed by **2**/H₂O₂ at room temperature ^a

Entry	Catalyst	Substrate	AcOH ^b	Yield (%) ^c	Phenol Selectivity (%)			Aliphatic Chain oxidation
					<i>ortho</i>	<i>meta</i>	<i>para</i>	
1	2	Benzene	-	14.0	-	-	-	-
2			1.0 eq	20.0	-	-	-	-
3	2	Toluene	-	12.1	33	25	25	Benzaldehyde (2.1%)
4			1.0 eq	26.0	46	15	30	Benzaldehyde (2.0%)
5	2	Ethylbenzene	-	11.0	23	-	41	1-Phenylethanol (4.0%)
6			1.0 eq	21.0	36	-	52	1-Phenylethanol (2.5%)
7	1^d	Benzene	-	10.0	-	-	-	-
8			1.0 eq	14.0	-	-	-	-

^a Reaction condition: **2** (1.0 mM), substrate (300 mM), H₂O₂ (10 mM) in acetonitrile at 298K, Reaction time 15 min (See experimental section for details). ^bAcOH (1.0 equiv. w.r.t. **2**) was added prior to the addition of H₂O₂; ^cYields are based on initial oxidant concentration; ^dreference 7a

15 min, the products have been acetylated by 1-methylimidazole/Ac₂O (as described elsewhere) before their identification and quantification by GC. Under this condition, phenol has been obtained in 14.0% yield based on the initial oxidant concentration along with *p*-quinone (< 1.0 %) as the minor product. Overall selectivity for phenol production has been estimated to be > 99.0% (Entry 1, Table 1). A slightly higher yield of phenol (20.0%) is obtained when the reaction is carried out in presence of acetic acid (1.0 equiv. w.r.t. **2**). As evident from Table 1, the diiron complex (**2**) emerges as a better catalyst compared to its monomeric congener (**1**) (Entry 7 & 8, Table 1) towards benzene hydroxylation under identical reaction condition.^{7a}

In order to gain further insight into the mechanism, toluene is used as the substrate. Toluene offers both aromatic and aliphatic C-H bonds with different bond strengths (88 kcal/mol for CH₂-H vs. 113.5 kcal/mol for *p*-H-C₆H₄Me).¹⁷ Preferential oxidation of aliphatic C-H bond in toluene indicates an initial hydrogen abstraction process, whereas, higher selectivity towards aromatic ring oxidation over aliphatic C-H oxidation suggests the involvement of highly electrophilic oxo-metal transient reacting with the arene π -system.¹⁸ In the present case, oxidation of toluene afforded the cresols as the main product (10% based on H₂O₂) along with 2.1% benzaldehyde (Entry 3, Table 1). This corresponds to 79% selectivity for ring oxidation. Moreover, in presence of acetic acid, **2**/H₂O₂ exhibited a clear preference towards ring hydroxylation over aliphatic hydroxylation (12:1) (Entry 4, Table 1) clearly indicating an electrophilic mechanism, presumably by a putative oxoiron(V) species operative during catalytic turnovers. Oxidation of ethylbenzene by **2**/H₂O₂ system also exhibits similar product profile (Entry 5 & 6, Table 1). **2**/H₂O₂ is found to oxidize ethylbenzene in 11% yield to a mixture of 2-ethylphenol, 4-ethylphenol and 1-phenylethanol. The ratio of products derived from aliphatic chain oxidation and aromatic

hydroxylation is found to be ca. 1:2. It is interesting to note that the monomeric iron(II) catalyst **1** with H₂O₂ was shown to promote preferential hydroxylation of methylene group than ring hydroxylation in ethylbenzene (1-phenylethanol/ethylphenols ~4:1) in absence of acetic acid additive.^{7a} Thus, the results indicate that somewhat different reaction pathways are operative in aromatic hydroxylation by **1**/H₂O₂ and **2**/H₂O₂.

Mechanistic aspect of aromatic hydroxylation

So far, only a limited number of nonheme iron-complexes have been reported to mediate aromatic hydroxylation with peroxides. In case of mononuclear iron(II) complexes bearing either N4 or N5 donors, high-valent oxo-iron species has been suggested as the active oxidant.^{6,7} The involvement of 'putative' iron(V)-oxo intermediates in arene hydroxylation is proposed independently by Banse *et al.*⁶ and Akimova *et al.*⁷ Recently, an Fe^{II} NHC complex is also shown to be effective in hydroxylation of benzene and toluene with hydrogen peroxide as the oxidant.⁹ Based on the observation of inverse KIE and high regio- and chemoselectivity observed, the authors argued in favour of an electrophilic attack by a high-valent Fe=O on the aromatic ring. Moreover, aromatic hydroxylation of the coordinated ligand is also observed in some cases, which emphasize the importance of positioning of the substrate near the oxo-metal transient.¹⁹ Interestingly, a triplet iron(IV)-oxo species is proposed as the key oxidant in intra-molecular aromatic hydroxylation by experimental and theoretical study. Given the fact that a vast majority of nonheme iron(IV)-oxo complexes exhibit sluggish reactivity,²⁰ the results provide significant insight regarding the role of secondary coordination sphere in modulating the reactivity of metal-oxygen intermediates. Therefore, despite some notable

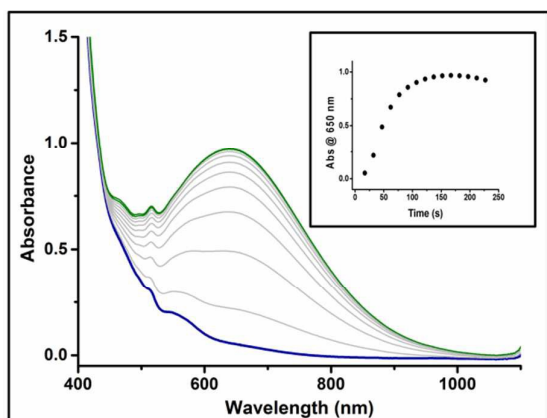


Fig. 1 UV-visible changes for the reaction of **2** (1.0 mM), benzene (300 mM) and H_2O_2 (10 mM) in acetonitrile at 298K. Blue line represent the initial UV-vis spectrum of the complex **2** and the green line represent the final spectrum of the iron(III)-phenolate species. Inset: Absorbance changes at 650 nm with time after the addition of H_2O_2

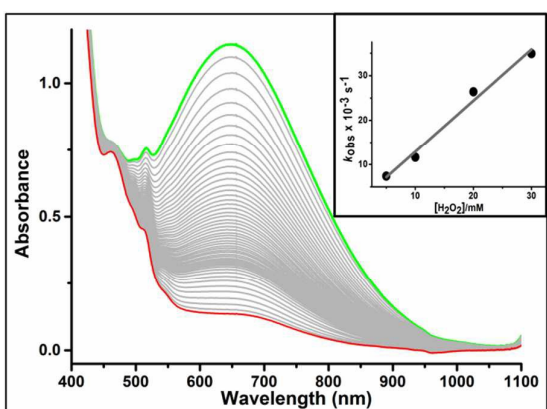


Fig. 2 Decay of the 650 nm band with time. The final spectrum corresponding to the $[(\text{bpmen})(\text{H}_2\text{O})\text{Fe}(\mu\text{-O})\text{Fe}(\text{OH})(\text{bpmen})]^{2+}$ (**2'**) complex is shown in red. Inset: The rate of formation of the iron(III) phenolate species in acetonitrile at 298K as a function of H_2O_2 concentration. The kinetic traces at 650 nm were fitted in a single-exponential decay profile. The pseudo-first order rate constants (k_{obs} , s^{-1}) were plotted against H_2O_2 concentration. From the linear plot, the second-order rate constant (k_2 , $\text{M}^{-1}\text{s}^{-1}$) was obtained.

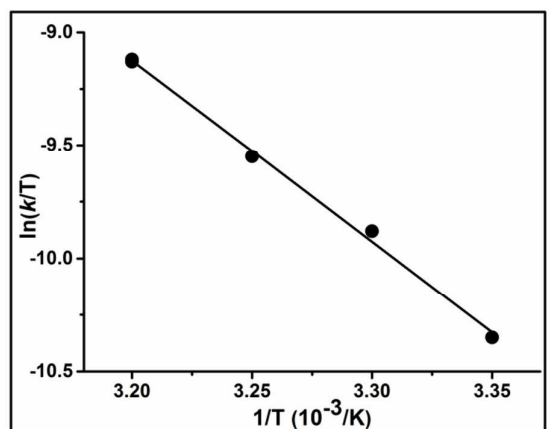
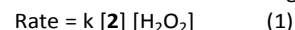


Fig. 3 Plot of first-order rate constants against $1/T$ to determine activation parameters.

results the mechanism of aromatic hydroxylation remains poorly understood. Moreover, aromatic hydroxylation mediated by oxo-bridged diiron(III) complexes is sparsely reported in the literature.^{10,21} The oxo-bridged diiron(III) complex based on an EDTA based ligand has been shown to

hydroxylate the coordinated phenyl ring.²¹ However, the diferric complex was found to disintegrate into a mononuclear(III) product at the end of the reaction. Very recently, Wang *et al.* has reported aromatic hydroxylation ability of $[\text{FeFe}]$ -hydrogenase model complexes with H_2O_2 .¹⁰ Based on computational and experimental studies, the authors have suggested the formation of a μ -oxo complex as the active intermediate for aromatic hydroxylation.

The results prompted us to explore the mechanism of arene hydroxylation by the complex $[(\text{bpmen})_2\text{Fe}_2\text{O}(\mu\text{-O})(\mu\text{-OH})(\text{ClO}_4)_3]$ (**2**) and H_2O_2 . Addition of 10 mM H_2O_2 to an acetonitrile solution of **2** (1 mM) containing 300 mM benzene results in the formation of a blue-green species ($\lambda=650$ nm), which, then slowly decays (Figure 1 & 2). The electronic spectral changes suggests the formation of phenolate-bound iron(III) species. Indeed, ESI-MS spectrum taken after the maximum accumulation of the species exhibited a peak centered at $m/z=478$, which can be assigned to $[(\text{bpmen})\text{Fe}^{\text{III}}(\text{OPh})(\text{OH})(\text{MeCN})+\text{H}]^+$ (Figure S1a, Supporting Information). The formation of the iron(III)-phenolate appears to follow a single-exponential growth profile and yields a pseudo first-order rate constant (k_{obs}) value of $8.0 \times 10^{-4} \text{ s}^{-1}$. The k_{obs} values have been found to be linearly dependent on the concentration of H_2O_2 allowing us to estimate the second-order rate constant (k_2) of $1.21 \text{ M}^{-1}\text{s}^{-1}$ (inset, Figure 2). Formation of the iron(III)-phenolate species is found to be independent of initial benzene concentration (Figure S2, ESI) Activation parameters for benzene hydroxylation were determined by plotting the first-order rate constants measured at different temperatures (298-313K) against $1/T$ (Figure 3); the activation enthalpy and entropy values were estimated to be $\Delta H^\ddagger = 66.6 \text{ kJmol}^{-1}$ and $\Delta S^\ddagger = -79.8 \text{ Jmol}^{-1}\text{K}^{-1}$. The high activation enthalpy and large negative activation entropy are consistent with a bimolecular rate-limiting step (Eq. 1).



The kinetics of benzene hydroxylation by **2**/ H_2O_2 differ significantly from the kinetic results obtained previously using nonheme iron(II) complexes with H_2O_2 in aromatic hydroxylation. The intermediacy a monomeric iron(III)-hydroperoxide species in aromatic hydroxylation by nonheme iron(II) complexes and H_2O_2 has previously been observed separately by Akimova *et al.* and Banse *et al.*^{6,7} The formation of the phenolate in these systems has been shown to follow a two-exponential process; the first process corresponds to the formation of iron(III)-hydroperoxide species whereas rate-determining formation of a true oxidant is believed to be associated with the second process. In the present investigation, linear dependence of rate on H_2O_2 concentration seems to exclude the formation of a mononuclear iron(III)-hydroperoxide species in the rate-determining step. To further confirm this hypothesis, we attempted to detect such species in aromatic hydroxylation by **2**/ H_2O_2 by UV-visible spectroscopy and *in situ* ESI-MS study. However, upon addition of H_2O_2 to an acetonitrile solution of **2** did not generate the monomeric the iron(III)-hydroperoxide in the temperature range of 0-25°C as evident from the absence of a characteristic bands in the range of 500-560 nm. Furthermore, no peaks

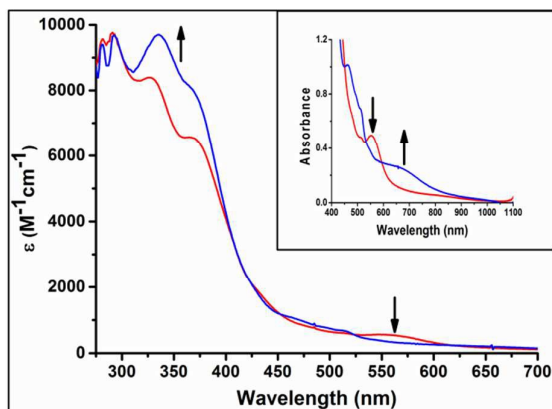
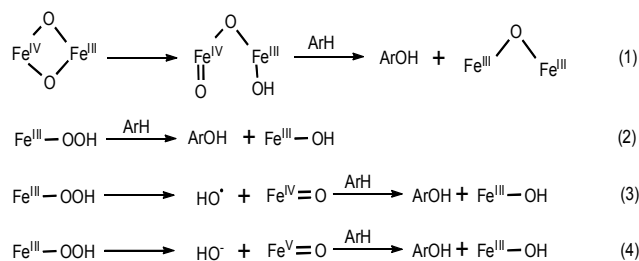


Fig. 3 UV-vis spectrum of the complex **2** (1.25×10^{-4} M) (red line) and that of the species obtained at the end of the aromatic hydroxylation (blue line) in dry acetonitrile at 298 K. The final spectrum corresponds to the complex $[(\text{bpmen})(\text{H}_2\text{O})\text{Fe}(\mu\text{-O})\text{Fe}(\text{OH})(\text{bpmen})]^{3+}$ (**2'**). Inset: Electronic spectra of **2** (1 mM) and **2'** in the visible region in dry acetonitrile at 298 K.

corresponding to this species is detected during the *in situ* ESI-MS analysis (Figure S1a, Supporting Information). The results are also consistent with the formation of phenolate-bound iron(III) following a single-exponential process in the present case (Figure 1 & 2). The results encouraged us to investigate the fate of the oxo-bridged diiron(III) core during catalytic aromatic hydroxylation. The electronic spectra obtained after the complete decay of the 650 nm is compared with that of the starting complex (**2**) in Figure 3. The final spectrum exhibits new bands around 350, 430 and 512 nm. The decay of the absorption band at 512 nm is indicative of the rupture of μ -oxo diiron motif during the reaction. However, the final spectrum is strikingly similar to that of $[(\text{bpmen})(\text{H}_2\text{O})\text{Fe}(\mu\text{-O})\text{Fe}(\text{OH})(\text{bpmen})]^{3+}$,²² previously observed by Poussereau *et al.* upon addition of water to an acetonitrile solution of complex **2**. Thus, it is reasonable to believe that the oxo-bridged diiron(III) (**2**) first dissociate in solution to form mononuclear species followed by the regeneration of the Fe(III)–(μ -O)–Fe(III) core after the catalytic turnovers. Interestingly, the final complex (**2'**) has been found to mediate further aromatic hydroxylation when a second batch of benzene (300 mM) and H_2O_2 was added at the end of the reaction. Formation of the 650 nm band is seen (Figure S3, Supporting Information) and the spectroscopic yield of the phenolate bound iron(III) is found to be comparable with that observed during the first addition.

The origin of the reactivity of the oxo-bridged diiron(III) complex (**2**) towards aromatic hydroxylation remains to be elucidated. However, preliminary studies undertaken in this work have revealed some interesting mechanistic puzzles. Firstly, the final complex obtained after catalytic aromatic hydroxylation by **2**/ H_2O_2 in acetonitrile has been found to contain (μ -O)diiron(III) structural motif. Secondly, the regenerated complex (**2'**) has been found to mediate hydroxylation of benzene with H_2O_2 .

In order to explain the results, we have considered several mechanistic hypotheses which are outlined below (eq. 1-4).



Scheme 2 Proposed mechanism for aromatic hydroxylation by **2**/ H_2O_2 .

Mechanistic work on the mechanism of toluene-4-monooxygenases have revealed that the diiron(III) resting state of the enzyme is first reduced by 2-electron transfer from an NADH-dependent reductase and the reaction between the resulting diiron(II) species with dioxygen results in the formation of a high-valent diiron(IV) species (Complex 'Q') which hydroxylates the aromatic ring of toluene via a rebound mechanism.^{5a} In recent years, structurally similar high-valent diiron species have been characterized. Que and coworkers identified a diamond core species, $\text{Fe}^{\text{III}}\text{Fe}^{\text{IV}}(\mu\text{-O})_2$ supported on a tripodal N4 ligand.²³ The species has been found to yield the valence-localized $[\text{OH}-\text{Fe}^{\text{III}}(\mu\text{-O})\text{Fe}^{\text{IV}}=\text{O}]$ species. The latter species featuring an S=2 terminal iron(IV)oxo has already been shown to be highly reactive in cleaving C-H bonds.²⁴ Based on these results, formation of similar high-valent diiron(III) species based on N4-bpmen ligands can be envisioned. However, in absence of literature precedence of the involvement of similar species in metal complex catalyzed aromatic hydroxylation, rigorous spectroscopic data is needed to substantiate the claim.

The second possibility indicating the involvement of a mononuclear ferric hydroperoxo species as the active oxidant is less likely to be true. A number of nonheme ferric hydroperoxo species have already been generated and characterized.²⁵ They have been found to be sluggish oxidants and therefore, less like to cleave C(aryl)-H bonds directly.²⁶ More recently, studies by Banse *et al.* have shown that the ferric hydroperoxo species undergo homolytic cleavage to generate more reactive iron(IV) oxo transients capable of cleaving C-H bonds.²⁷ However, in aromatic hydroxylation by **2**/ H_2O_2 , this possibility can be safely excluded on the basis of the lack of reactivity of independently generated $[\text{Fe}^{\text{IV}}(\text{O})\text{bpmen}]$ towards C(aryl)-H bonds.^{7a}

The fourth scenario considers the heterolytic cleavage of the peroxy linkage in Fe(III)-OOH to generate a 'putative' iron(V) oxo species. Although similar iron(V) oxo species have rarely been detected,²⁸ theoretical studies have indicated their superior oxidative reactivity in cleaving strong C-H bonds.²⁹ Moreover, involvement of high-valent oxoiron(V) intermediate has previously been proposed for benzene hydroxylation by monomeric $[\text{Fe}^{\text{II}}(\text{bpmen})]^{2+}$ (**1**) and H_2O_2 by Akimova and coworkers.^{7a} In the present case, arene hydroxylating ability of complex **2** and H_2O_2 can be explained considering spontaneous dissociation of the diiron(III) complex into a monomeric ferric

complex. Additional supports for this hypothesis have been obtained from EPR studies. The starting diiron(III) complex (**2**) is EPR silent due to the presence of two antiferromagnetically coupled Fe(III) centres. Addition of 10 equiv. of H₂O₂ to an acetonitrile solution of complex **2** (1 mM) at room temperature and freezing the mixture at -78°C, the EPR spectrum (Figure S4, ESI) is found to exhibit a signal at $g = 4.23$, which can be tentatively assigned to a high-spin mononuclear iron(III) complex. Moreover, the spectrum also indicates the presence of at least two $S=1/2$ species in the mixture (Figure S4). The resonances at $g_1 = 2.15$, $g_2 = 2.15$ and $g_3 = 2.08$ can be rationalized either by considering the formation of a low-spin ferric hydroperoxo intermediate or a binuclear Fe^{IV}Fe^{III} complex with antiferromagnetically coupled Fe^{III} ($S = 3/2$) and a low-spin Fe^{IV} ($S=1$) unit.³⁰ The second set of signals appears at $g_1 = 2.06$, $g_2 = 2.01$ and $g_3 = 1.96$. Both the $S=1/2$ signals have been found to decay with time. It is noteworthy that an $S=1/2$ EPR signal similar to the latter has recently been detected by Talsi *et al.* in reactions between structurally related oxo-bridged diiron(III) complex and H₂O₂ at low temperature.¹³ The EPR spectrum obtained after the addition of excess benzene to **2**/H₂O₂ mixture (Figure S4, ESI) exhibit a $S=3/2$ signal at 4.26, which can be assigned to the phenolate-bound iron(III) complex. A broad $S=1/2$ signal is also observed in this case. The formation of mononuclear species is also evident from the in situ ESI-MS study. ESIMS spectrum obtained after addition of H₂O₂ to an acetonitrile solution of **2** (1 mM) and excess benzene (Figure S1a & S1b, ESI), exhibits prominent peaks at $m/z=342$, 361 and 478. The first two peaks are assignable to [(bpmen)Fe^{III}(O)]⁺ and [(bpmen)Fe^{III}(O)(OH₂)]⁺. The peak at $m/z=478$ corresponds to the phenolate-bound iron(III) species, [(bpmen)Fe^{III}(OPh)(OH)(MeCN)+H]⁺. Based on these experimental observations, the arene hydroxylating ability of **2**/H₂O₂ can be rationalized by considering the dissociation of diiron(III) complex (**2**) to generate a monomeric high-spin iron(III) species. This step is followed by the formation of a transient ferric hydroperoxo species. Heterolysis of the O-O bond in the ferric hydroperoxo complex is believed to generate a 'putative' oxoiron(V) intermediate capable of oxidizing C(aryl)-H bonds.

Conclusions

In conclusion, we report the aromatic hydroxylation of benzene and alkylbenzenes by a nonheme diiron(III) complex [(bpmen)₂Fe₂O(μ-O)(μ-OH)](ClO₄)₃ (**2**) with H₂O₂ as the oxidant at room temperature. No intermediate mononuclear iron(III)-hydroperoxide is detected during arene hydroxylation. The rate of aromatic hydroxylation has been found to depend on initial concentration of H₂O₂. The results indicate that the reactivity of the diferric complex (**2**) differs significantly from that of its monomeric congener (**1**). High selectivity towards aromatic ring oxidation over the alkyl chain oxidation in toluene and ethylbenzene suggest the involvement of electrophilic high-valent oxoiron species as the true oxidant. The μ-oxo diiron(III) core in complex **2** is found to be

regenerated after the catalytic turnovers. The diiron(III) complex first dissociates in solution to form a mononuclear iron(III) species, which ultimately generates highly reactive oxoiron(V) intermediate capable of oxidizing aromatic C-H bonds. Although, the aromatic hydroxylation mitigates through monoiron species, regeneration of the μ-oxo diiron(III) core at the end of the catalytic turnover makes the diiron(III) complex (**2**) a *functional mimic* of toluene monooxygenases (TMOs). The results reported in this study are believed to stimulate further research aimed at the unambiguous identification of the key high-valent oxoiron transients.

Acknowledgements

The financial support from SERB (SR/S1/IC-53/2010), DST, Government of India are gratefully acknowledged. We thank CSIR (India) for the award of fellowship to AK.

Notes and references

- (a) Z. Long, Y. Zhou, G. Chen, P. Zhao, J. Wang, *Chem. Eng. J.*, 2014, **239**, 19; (b) D.A. Alonso, C. Najera, I.M. Pastor, M. Yus, *Chem. Eur. J.*, 2010, **16**, 5274; (c) S. Niwa, M. Eswaremoorthy, J. Nair, A. Raj, N. Itoh, H. Shoji, T. Namba, F. Mizukami, *Science*, 2002, **295**, 105; (d) X. Chen, J. Zhang, X. Fu, M. Antonietti, X. Wang, *J. Am. Chem. Soc.*, 2009, **131**, 11658; (e) O. Shoji, T. Kunimatsu, N. Kawakami, Y. Watanabe, *Angew. Chem. Int. Ed.*, 2013, **52**, 6606; (f) B. Lücke, K.V. Narayana, A. Martin, K. Jähnisch, *Adv. Synth. Catal.*, 2004, **346**, 1407.
- (a) J.H. Tyman, *Synthetic and natural phenols*, Elsevier, Amsterdam, 1996; (b) V.M. Zakoshansky, *Petroleum Chemistry*, 2007, **47**, 273. (c) M. Weber, M. Weber, M. Kleine-Boymann, In *Ullmann's Encyclopedia of Industrial Chemistry*, Wiley-VCH, Weinheim, Germany, 2000.
- R.J. Schmidt, *Appl. Catal. A*, 2005, **280**, 89.
- B. Cornils, W.A. Herrmann, *J. Catal.*, 2003, **216**, 23.
- (a) R. Ullrich, M. Hofrichter, *Cell. Mol. Life. Sci.*, 2007, **64**, 271; (b) Y. Tao, A. Fishman, W.E. Bentley, T.K. Wood, *J. Bacteriol.*, 2004, **186**, 4705; (c) M.H. Sazinsky, J. Bard, A. Di Donato, S.J. Lippard, *J. Biol. Chem.*, 2004, **279**, 30600; (d)
- (a) A. Thibon, V. Jollet, C. Ribal, K. Senechal-David, L. Billon, A.B. Sorokin, F. Banse, *Chem. Eur. J.*, 2012, **18**, 2712; (b) A. Thibon, J.-F. Bartoli, R. Guillot, J. Sainon, m. Martinho, D. Mansuy, F. Banse, *J. Mol. Catal. A:Chem.*, 2008, **287**, 115; (c) D. Mathieu, J.-F. Bartoli, P. Battioni, D. Mansuy, *Tetrahedron*, 2004, **60**, 3855; (d) V. Balland, D. Mathieu, N. Pons-Y-moll, J.-F. Bartoli, F. Banse, P. Battioni, J.-J. Girerd, D. Mansuy, *J. Mol. Catal. A: Chem.*, 2004, **215**, 81.
- (a) O.V. Makhlynets, E.V. Rybak-Akimova, *Chem. Eur. J.*, 2010, **16**, 13995; (b) S. Taktak, M. Flook, B.M. Foxman, L. Que, Jr., E.V. Rybak-Akimova, *Chem. Commun.*, 2005, 5301; (c) O.V. Makhlynets, W.N. Oloo, Y.S. Moroz, I.G. Belaya, T.D. Palluccio, A.S. Filatov, P. Müller, M.A. Cranswick, L. Que, Jr., E.V. Rybak-Akimova, *Chem. Commun.*, 2014, **50**, 645.
- S.P. de Visser, K. Oh, A.-R. Han, W. Nam, *Inorg. Chem.*, 2007, **46**, 4632.
- A. Raba, M. Cokoja, W.A. Herrman, F.E. Kühn, *Chem. Commun.*, 2014, **50**, 11454.
- X. Wang, T. Zhang, Q. Yang, S. Jiang, B. Li, *Eur. J. Inorg. Chem.*, 2015, 817.
- (a) O.Y. Lyakin, R.V. Ottenbacher, K.P. Bryliakov, E.P. Talsi, *ACS Catal.*, 2012, **2**, 1196; (b) O.Y. Lyakin, K.P. Bryliakov, G.J.P. Britovsek, E.P. Talsi, *J. Am. Chem. Soc.*, 2009, **131**,

- 10798; (c) O.Y. Lyakin, K.P. Bryliakov, E.P. Talsi, *Inorg. Chem.*, 2011, **50**, 5526.
- 12 W.N. Oloo, K.K. Meier, Y. Wang, S. Shaik, E. Münck, L. Que, Jr., *Nat. Commun.*, 2014, **5**, 3046.
- 13 O.Y. Lyakin, A.M. Zima, D.G. Samsonenko, K.P. Bryliakov, E.P. Talsi, *ACS Catal.*, 2015, **5**, 2702.
- 14 W.L.F. Armarego, D.D. Perrin, *Purification of Laboratory Chemicals*, 4th Ed., Pergamon Press, Oxford, England, 1997.
- 15 A. Iturrospe, B. Artetxe, S. Reinoso, L.S. Felices, P. Vitoria, L. Lezama, J.M. Gutiérrez-Zorrilla, *Inorg. Chem.*, 2013, **52**, 3084.
- 16 (a) A. Hazell, K. B. Jensen, C. J. McKenzie and H. Toftlund, *Inorg. Chem.*, 1994, **33**, 3127; (b) S.Taktak, S.V. Kryatov and E.V. Rybak-Akimova, *Inorg. Chem.*, 2004, **43**, 7196.
- 17 Y. R. Luo, *Comprehensive handbook of chemical bond energies*, CRC Press, Boca Raton, 2007.
- 18 S. P. de Visser, L. Tahsini, W. Nam, *Chem. Eur. J.*, 2009, **15**, 5577.
- 19 S. Sahu, L.R. Widger, M.G. Quesne, S.P. De Visser, H. Matsumara, P. Moënné-Locco, M.A. Siegler, D.P. **Goldberg**, *J. Am. Chem. Soc.*, 2013, **135**, 10590.
- 20 A.R. McDonald, L. Que, Jr., *Coord. Chem. Rev.*, 2013, **257**, 414.
- 21 S. Ménage, J.-B. Galey, G. Hussler, M. Seité, M. Fontecave, *Angew. Chem. Int. Ed.*, 1996, **35**, 2353.
- 22 S. Poussereau, G. Blodin, M. Cesario, J. Guilhem, G. Chottard, F. Gonnet, J.-J. Girerd, *Inorg. Chem.*, 1998, **37**, 3127.
- 23 (a) L. Que, Jr., W.B. Tolman, *Angew. Chem. Int. Ed.*, 2002, **41**, 1114; (b) S.V. Kryatov, E.V. Rybak-Akimova, *J. Chem. Soc., Dalton Trans.*, 1999, 3335.
- 24 (c) G. Xue, R. De Hont, E. Münck, L. Que, Jr., *Nature Chem.*, 2010, **2**, 400; A mononuclear S=2 iron(IV) complex with very high reactivity towards C-H bonds has recently been reported. See A.N. Biswas, M. Puri, K.K. Meier, W.N. Oloo, G.T. Rohde, E.L. Bominaar, E. Münck, L. Que, Jr., *J. Am. Chem. Soc.*, 2015, **137**, 2428.
- 25 (a) C. Kim, K. Chen, J. Kim, L. Que Jr., *J. Am. Chem. Soc.*, 1997, **119**, 5964. (b) R. Y. N. Ho, G. Roelfes, B. L. Feringa, L. Que, Jr., *J. Am. Chem. Soc.*, 1999, **121**, 264.
- 26 M. J. Park, J. Lee, Y. Suh, J. Kim, W. Nam, *J. Am. Chem. Soc.*, 2006, **128**, 2630.
- 27 A. S. Faponle, M. G. Quesne, C. V. Sastri, F. Banse, S. P. de Visser, *Chem. Eur. J.*, 2015, **21**, 1221
- 28 F. T. de Oliveira, A. Chanda, D. Banerjee, X. Shan, S. Mondal, L. Que, Jr., E. L. Bominaar, E. Münck, J. T. Collins, *Science* 2007, **315**, 835. (b) O. Y. Lyakin, K. P. Bryliakov, G. J. P. Britovsek, E. P. Talsi, *J. Am. Chem. Soc.* 2009, **131**, 10798.
- 29 (a) A. Bassan, M. R. A. Blomberg, P. E. M. Siegbahn, L. Que, Jr., *Chem. Eur. J.*, 2005, **11**, 692. (b) P. Comba, M. Maurer, P. Vadivelu, *J. Phys. Chem. A.*, 2008, **112**, 13028. (c) S. Chakrabarty, R. N. Austin, D. Deng, J. T. Groves, J. D. Lipscomb, *J. Am. Chem. Soc.* 2007, **129**, 3514.
- 30 (a) E.A. Duban, K.P. Bryliakov, E.P. Talsi, *Eur. J. Inorg. Chem.*, 2007, 852; (b) E.A. Duban, K.P. Bryliakov, E.P. Talsi, *Kinet. Catal.*, 2008, **49**, 379.

Electronic Supporting Information

Aromatic Hydroxylation by an Oxo-bridged Diiron(III) Complex: A Bio-inspired Functional Model of *Toluene Monooxygenases*Ambica Kejriwal,^a and Pinaki Bandyopadhyay^a and Achintesh N. Biswas^{*b}

^a Department of Chemistry, University of North Bengal, Raja Rammohunpur, Siliguri 734013, India. Fax: 91 353 2699001; Tel: 91 353 277684; E-mail: pbchem@rediffmail.com

^b Department of Chemistry, Siliguri College, Siliguri 734001, India; E-mail: achintesh@gmail.com

Contents

- Figure S1a. ESIMS spectrum obtained during the course of benzene hydroxylation by **2**/H₂O₂.
- Figure S1b. Experimental and theoretical isotope distribution patterns. The peak at m/z = 342 has been assigned to [(bpmen)Fe^{III}(O)]⁺ whereas the peak at m/z = 361 can be assigned to the species [{(bpmen)Fe^{III}(O)(OH₂)}+H]⁺. The peak at m/z = 478 can be assigned to [(bpmen)Fe^{III}(OPh)(OH)(MeCN)+H]⁺.
- Figure S2. Rate of formation of phenolate as a function of benzene concentration
- Figure S3. Electronic changes observed after the addition of additional H₂O₂ (10 mM) to the final diiron(III) complex (black line). The final spectrum corresponding to the phenolate bound iron(III) species is shown in green.
- Figure S4. Rate of formation of phenolate as a function of benzene concentration.
- Figure S4. X-band EPR spectrum obtained after the addition of 10 mM H₂O₂ to an acetonitrile solution of **2** (1.0 mM) at 298 K followed by rapid freezing of the solution (red line). EPR spectrum obtained after the addition of 10 mM H₂O₂ to an acetonitrile solution of **2** (1.0 mM) and benzene (300 mM) at 298 K followed by rapid freezing of the solution (black line).

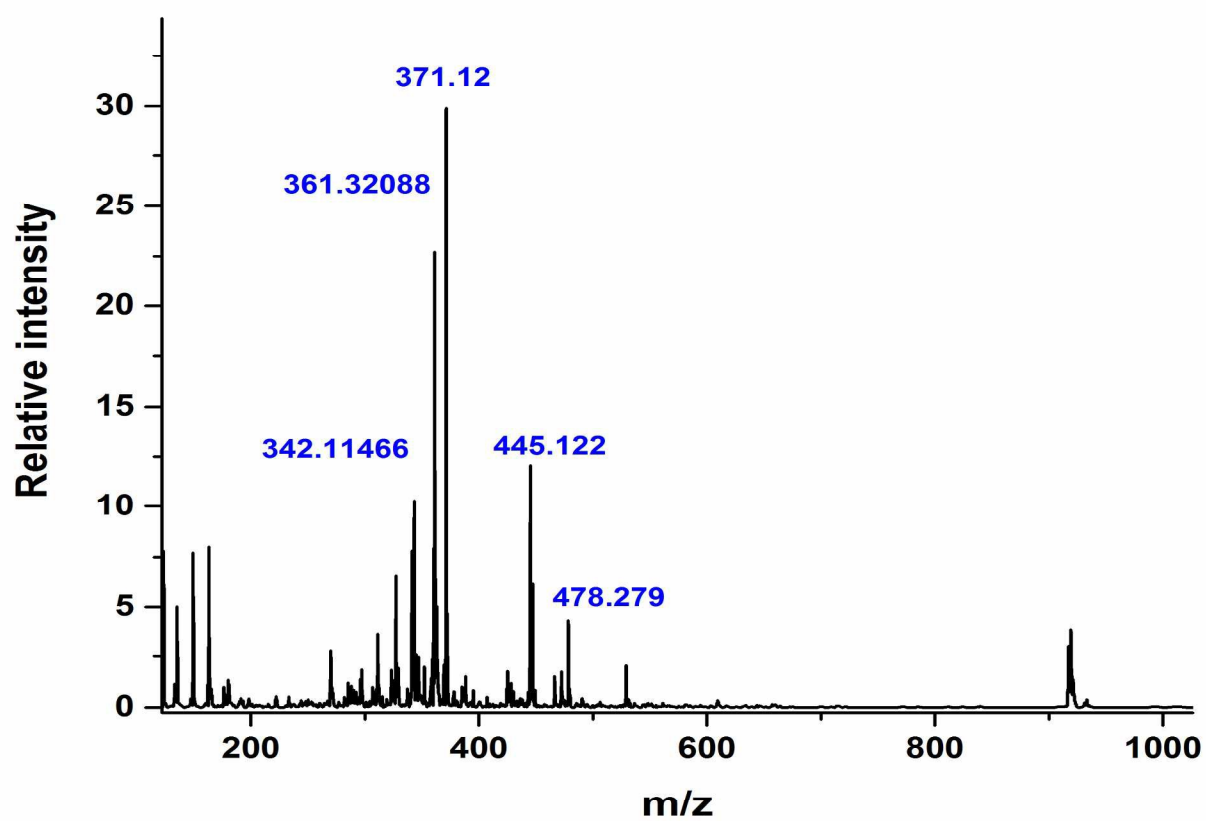


Figure S1a. ESIMS spectrum obtained during the course of benzene hydroxylation by **2**/H₂O₂.

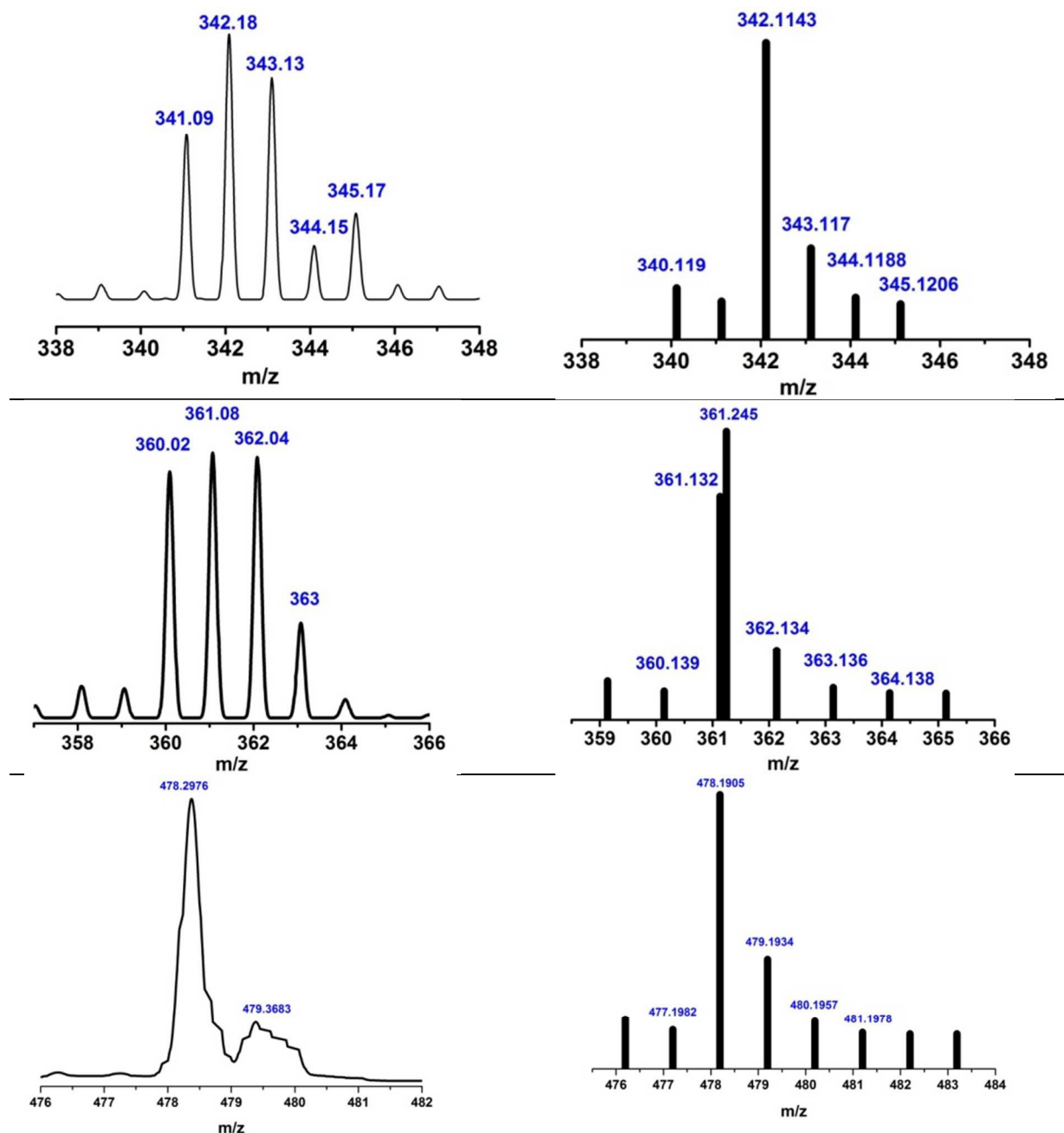


Figure S1b. Experimental and theoretical isotope distribution patterns. The peak at $m/z = 342$ has been assigned to $[(\text{bpmen})\text{Fe}^{\text{III}}(\text{O})]^+$ whereas the peak at $m/z = 361$ can be assigned to the species $[(\text{bpmen})\text{Fe}^{\text{III}}(\text{O})(\text{OH}_2)]^+$. The peak at $m/z = 478$ can be assigned to $[(\text{bpmen})\text{Fe}^{\text{III}}(\text{OPh})(\text{OH})(\text{MeCN})]^+$.

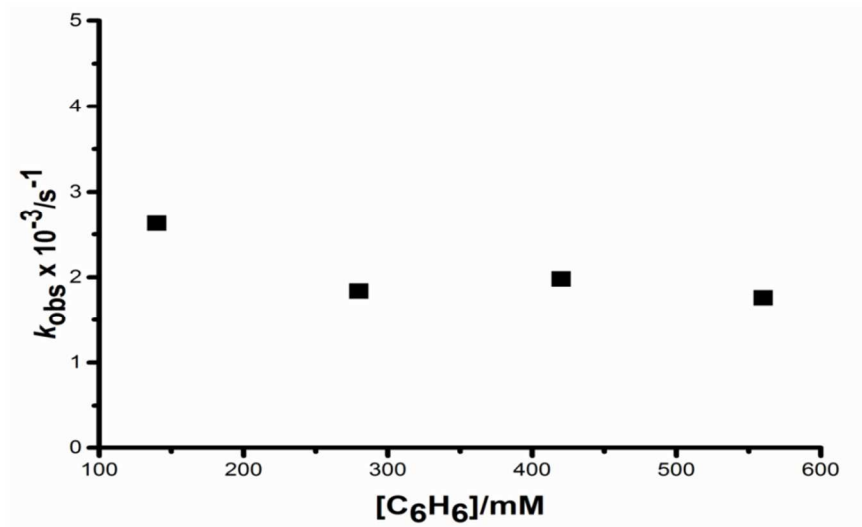


Figure S2. Rate of formation of phenolate as a function of benzene concentration.

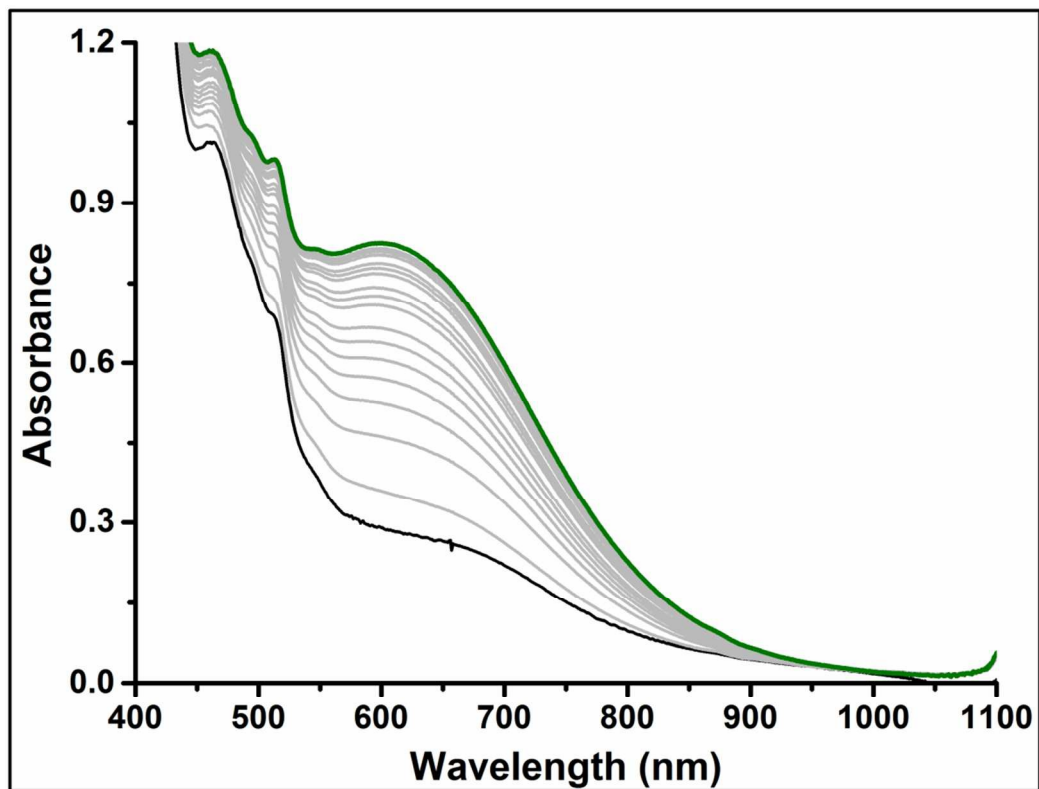


Figure S3. Electronic changes observed after the addition of additional H₂O₂ (10 mM) to the final diiron(III) complex (black line). The final spectrum corresponding to the phenolate bound iron(III) species is shown in green.

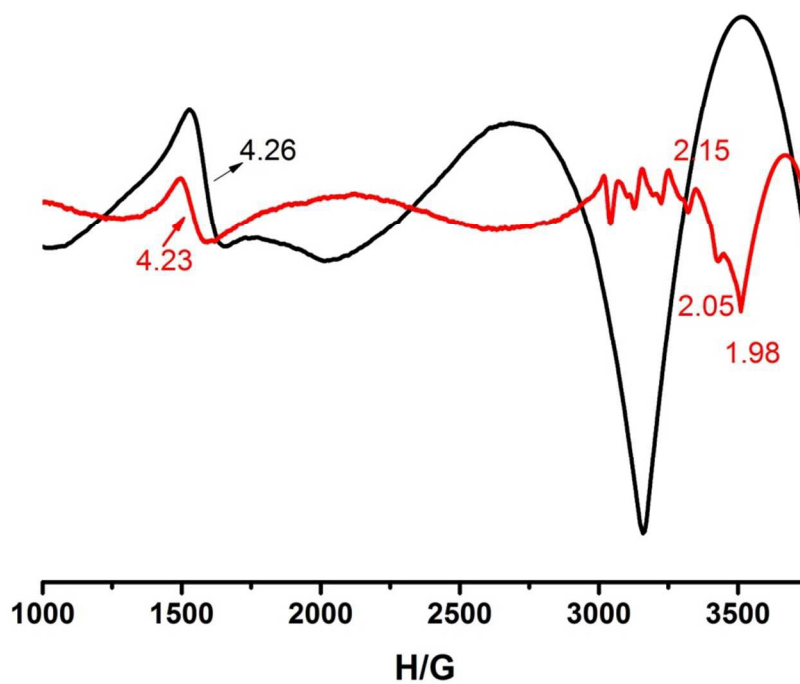


Figure S4. X-band EPR spectrum obtained after the addition of 10 mM H_2O_2 to an acetonitrile solution of **2** (1.0 mM) at 298 K followed by rapid freezing of the solution (red line). EPR spectrum obtained after the addition of 10 mM H_2O_2 to an acetonitrile solution of **2** (1.0 mM) and benzene (300 mM) at 298 K followed by rapid freezing of the solution (black line).